Contents lists available at Sjournals

Health, Safety and Environment

Original article

Modeling and simulation to predict nitrogen deposition influenced by the porosity and the coefficient of inhibition in the coastal area of port Harcourt, Niger delta of Nigeria

S.N. Eluozo

Subaka Nigeria Limited Port Harcourt; Civil and Environmental Engineering Consultant Department of Research and Development, Rivers State of Nigeria.

[*]Corresponding author; Subaka Nigeria Limited Port Harcourt; Civil and Environmental Engineering Consultant Department of Research and Development, Rivers State of Nigeria.

ARTICLE INFO

ABSTRACT

Nitrogen deposition influenced by porosity and coefficient of inhibition has been thoroughly evaluated. This study were carried out to monitor the deposition of nitrogen at various formation in coastal area of Port Harcourt, the model developed theoretical values, the values where compared with experimental values, both parameters generated a best fit, the results from the figures presented shows that the deposition of nitrogen where found to be on exponential phase, the lowest were found to deposit at three metre at the period of ten days, while that highest were recorded at thirty metres at the period of hundred days, the developed model from the values shows the rate of influences from degree of porosity. The rate of deposition at aquiferious zone shows the extent it will increase the microbial population to ground water aquifers in the study location. The rate of concentration at aquiferious zone are determine by the degree of porosity in ground water aquifers, because the highest concentration from the figures present were found to deposit the highest concentration within the gravel and coarse formation where ground water aquifers are deposited, the study are imperative because it will be applied to monitor the deposition of substrate utilization at aquiferious zone.

1. Introduction

Soil water establishment is highly affected by soil formation and its steadiness. Various soil arrangement types may cause preferential flow or water immobilization (Kodešová *et al.,* 2006, 2007, 2008). Soil structure breakdown may initiate a soil particle migration, formation of less porous or even water-resistant layers and as a result of decreased water fluxes within the soil profile (Kodešová *et al.,* 2009a). Soil aggregation is under managed of different mechanisms in different soil types and horizons (Kodešová *et al.,* 2009b). Soil formation and consequently soil hydraulic properties of tilled soil varied in space and time (Strudley *et al.,* 2008). The temporal variability of the soil aggregate stability was shown for instance by Chan *et al.* (1994), and Yang and Wander (1998). While Chan *et al*. (1994) documented that temporal changes of aggregate stability were not positively related to living root length density; Yang and Wander (1998) suggested that the higher aggregate stability was found due to crop roots, exudates microbial by-products and wet/dry cycles. The temporal variability of the soil hydraulic properties (mainly hydraulic conductivities, K) were investigated, for instance in following studies. Murphy *et al*. (1993) showed that K values at tensions of 10 and 40 mm varied temporally due to the tillage, wetting/drying, and plant growth. Messing and Jarvis (1993) presented that the K values decreased during the growing season due to the structural breakdown by rain and surface sealing. Somaratne and Smettem (1993) documented that while the K values at tension of 20 mm were reduced due to the raindrop impact, the K values at tension of 40 mm were not influenced. Angulo-Jaramillo, *et al*. (1997) discovered that only the more homogeneous sandy soil under furrow irrigation exhibited significant decrease in sorptivity. Petersen *et al*. (1997) documented using the dye tracer experiment that cultivation reduced the number of active preferential flow paths. Azevedo *et al*. (1998) measured tension infiltration from 0 to 90 mm and showed that macropore flow decreased from 69% in July to 44% in September. Bodner *et al.* (2008) discussed the impact of the rainfall intensity, soil drying and frost on the seasonal changes of soil hydraulic properties in the structure-related range. Finally, Suwardji and Eberbach (1998) studied both, aggregate stability and hydraulic conductivities. They documented the lowest aggregate stability during the winter and increased in spring. The K values decreased during the growing season. The goal of this study is to assess the seasonal variability of the soil structure, aggregate stability and hydraulic properties with respect to each other and to varying soil physical and chemical properties, soil management and climatic conditions

2. Materials and methods

2.1. Experiment set up

The column was set up; the height is 1 metre of 10mm diameter steel pipe, positioned at vertical level, including a funnel of 30cm that contains 4 litres of waste water. Each sample level of average of 2000mg/l of waste water containing *E. coli* was poured inside the column. While the flow was passing through the column, a stop watch was used to monitor the speed level, to determine the level of transport of each sample of aquifer materials. The effluent 1000mg/l from the column were collected and subjected to thorough analysis to determine the level of transport of *E. coli* in each of the aquifer material s, which determines the level of transport to aquiferous zone.

2.2. Bacteriological testing of water

Methodology: Membrane filtration. (WHO, 1993, 1996, 1998)
Principle of the method: A 100ml water sample was filtered through membrane filters. The membranes, with the coliform organism (*E. coli*) on it, are then cultured on a pad of sterile selective broth containing lactose and an indicator. After incubation, the number of colonies of coliform (*E. coli*) were counted. This gives the presumptive number of *E. coli* in the 100ml water sample.
 Choice of technique: The method is recommended for its accuracy, speed of result, and because it can be performed in the field.

Required

1. Sterile filtration unit for holding 47mm diameter membrane filters with suction device (wagteck international)
2. Sterile grid membrane filters of 47mm diameter with a pore size of 0.45um (oxide).
3. Sterile 47mm diameter cellulose pads (both culture medium to be added just before use).
4. Sterile Petri dishes 50-60mm diameter
5. Sterile membrane lauryl sulphate broth (lactose sodium lauryl sulphate broth)

Autoclaving unit, blunt ended forceps, sterile bottles, grease pencil, incubator at 44°c, Bunsen burner, Petri-dish holders and oblique light source

Procedure

a. Assembling the filtration unit: The sterile broth is aseptically added to the cellulose pad in a Petri-dish. The membrane filter is aseptically removed from the sterile pack using a flame sterilized blunt forceps and placed on the filter base with the grid-side uppermost and centrally. Next, the filter lid was screwed into place.
b. Suction Filtration of water sample: 100ml of the different water samples were thoroughly mixed by inverting the bottles several times and gently poured into the assembled filtration unit.
- The water was drawn into the filter membrane by suction using the hand held pressure pump.
- A blunt-ended forceps was sterilized by naked Bunsen flame, cooled and the membranes were aseptically removed from the filtration unit after unscrewing the lid of the filtration unit.
- The membranes were placed, grid-side uppermost, on the culture medium pads in the Petri-dishes, ensuring there were no air bubbles trapped under the membranes.
- The Petri-dishes were closed and the top of the lids were labeled with the code numbers of the water samples and volumes of water used using a grease pencil.
Incubation of Samples:
- The Petri-dishes were packed in Petri dish holders with lids uppermost and placed inside the incubator at 44°c for 12 – 16 hours.
Examination, count and calculation of *E.coli* colonies:
- Following incubation and using oblique lighting, the membranes were examined one after the other for yellow lactose fermenting colonies, 1-3mm in diameter. The number of colonies if any was counted. Any plink and small colonies less than 1mm in diameter were ignored. Number of colonies too numerous to count were reported as "too numerous to count" (indicative of gross contamination).
- To calculate the presumptive *E. coli* count/100ml water sample, the number of colonies counted per membrane was multiplied by 1.

2.3. Nitrogen determination

Reagents

1. Nitrogen standards: Stock solution (1ml = NH_4^+ - N) prepare as for distillation. Working standard (1ml = 0.001mg NH_4^+ - N) dilute the stock solution 100 times. Prepare fresh each day.
2. Sodium hydroxide, 40% w/v.
3. Sodium phenate reagent: Dissolve 50 phenols in 250ml 40% NaOH and dilute to 400ml with water. Prepare fresh each day.
4. Rochelle reagent: Dissolve 60g sodium potassium tartrate (Rochelle salt) in water and dilute to 600ml with water.
5. Sodium nitroprusside, 0.16% w/v.
6. Sodium hypochlorite solution, 5% available Cl.

Procedure

1. Pipette 0 to 10ml working standard into 50ml volumetric flask to give a range from 0 to 0.01mg NH_4^+ - N.
2. Add blank acid digest to match the sample aliquots.
3. Pipette not more than 10ml sample digest into a 50ml volumetric flask.
4. From this point treat standards and samples in the same way.

5.   Add 8ml alkaline Rochelle reagent and mix.
6.   Add 1ml Na nitroprusside solution and mix.
7.   Add 2ml sodium phenate reagent and mix.
8.   Add 1ml sodium hypochlorite reagent, dilute to volume and mix well.
9.   Leave 20 minutes in a water bath at 40^{0}C, and then cool.
10.   Measure the optical density at 625nm or use an orange filter, using water as a reference.
11.   Prepare a calibration curve from the standard values and use it to obtain mg NH_4^+ - N in the sample aliquot.
12.   Carry out blank determination in the same way and subtract where necessary.

2.4. Calculation

If C = mg NH_4^+ - obtained from the graph then for:

N (%) = $\dfrac{C(mg) \times solution\ \ volume\ \ (ml)}{10 \times aliquot\ \ (ml)\ sample\ \ wt\ (g)}$

Governing equation

Nomenclature

Kc	=	Inhibitors
V	=	Velocity of Transport
Ks	=	Nitrogen Deposition
Q	=	Porosity of soil
T	=	Time of distance travel
X	=	Distance

$$V\frac{\partial Ks}{\partial t} = \phi\frac{\partial Ks}{\partial x} + Kc \qquad \text{.....................................} \qquad (1)$$

$$Ks = TZ$$

$$\frac{\partial Ks}{\partial t} = T^1 Z \qquad \text{.....................................} \qquad (2)$$

$$\frac{\partial Ks}{\partial X} = TZ^1 \qquad \text{.....................................} \qquad (3)$$

$$V\frac{T^1 Z}{TZ} = \phi\frac{T^1 Z}{TZ} + Kc = -\lambda^2 \qquad \text{.....................................} \qquad (4)$$

$$V\frac{T^1}{T} = \phi\frac{Z^1}{Z} + Kc = -\lambda^2 \qquad \text{.....................................} \qquad (5)$$

$$V\frac{T^1}{T} = -\lambda^2 \qquad \text{.....................................} \qquad (6)$$

$$\phi\frac{Z^1}{Z} + Kc = -\lambda^2 \qquad \text{.....................................} \qquad (7)$$

From (7) $T^1 + \dfrac{\lambda^2 T}{V} = 0$

$$Z = A\,Cos\frac{\lambda^2}{\sqrt{V}}t + B\,Sin\frac{\lambda^2}{\sqrt{V}}t \qquad \text{.....................................} \qquad (8)$$

From (6) $\phi\dfrac{Z^1}{Z} + Kc - \lambda^2 \qquad \text{.....................................} \qquad (9)$

$$\frac{Z^1}{Z} = \frac{-\lambda^2}{\phi Kc} \qquad \text{.....................................} \qquad (10)$$

By direct integration

$$LnT = \frac{\lambda^2}{\phi Kc} Z \qquad \text{.....................................} \qquad (11)$$

$$Z = D\ell^{\frac{-\lambda^2}{\phi Kc}Z} \qquad \text{.....................................} \qquad (12)$$

Combining (8) and (9) yields

$$Ks(Z,t) = \left[A\,Cos\,\frac{\lambda}{\sqrt{V}}t + B\,Sin\,\frac{\lambda}{\sqrt{\phi Kc}}Z \right] D\ell^{\frac{-\lambda^2}{\phi Kc}Z} \quad \text{..............} \qquad (13)$$

$$At = 0 \; K(o) = h_{AO}$$

$$Kso = A\,Cos\,\frac{\lambda}{\sqrt{V}}t + B\,Sin\,\frac{\lambda}{\sqrt{\phi Kc}}Z \qquad \text{................} \qquad \text{...............} \qquad (14)$$

$$\frac{\partial Ks}{\partial t}\bigg|_{t\,=\,0,B} = 0 \qquad \text{................} \qquad \text{.....................} \qquad (15)$$

$$From\,(13)\; \frac{\partial Ks}{\partial t} = \left[-A\frac{\lambda}{\sqrt{V}}\,Sin\,\frac{\lambda}{\sqrt{V}}t + B\frac{\lambda}{\sqrt{V}}\,Cos\,\frac{\lambda}{\sqrt{V}}t \right] D\ell^{\frac{-\lambda^2}{\phi Kc}Z} \text{.......} \qquad (16)$$

$$At\; t = 0$$

$$0 = B\frac{\lambda}{\sqrt{V}}D\ell^{\frac{-\lambda^2}{\phi Kc}Z} \Rightarrow B = 0\,D \neq 0 \qquad \text{................} \qquad \text{...............} \qquad (17)$$

$$Ks = \left[A\,Cos\,\frac{\lambda}{\sqrt{V}} \right] D\ell^{\frac{-\lambda^2}{\phi Kc}Z} \qquad \text{...............} \qquad \text{...............} \qquad (18)$$

$$Ks = AD\,Cos\,\frac{\lambda}{\sqrt{V}}t\;\ell^{\frac{-\lambda^2}{\phi Kc}Z} \qquad \text{................} \qquad \text{...............} \qquad (19)$$

$$\frac{\partial Ks}{\partial t} = \frac{AD\lambda}{\sqrt{V}}\,Sin\,\frac{\lambda}{\sqrt{V}}t\;\ell^{\frac{-\lambda^2}{\phi Kc}Z} \qquad \text{................} \qquad \text{..............} \qquad (20)$$

$$At\; t = \frac{\partial Ks}{\partial t} = 0$$

$$0 = \frac{-AD\lambda}{\sqrt{V}}\,Sin\,\frac{\lambda d}{\sqrt{V}} = n\pi = \frac{\lambda\partial}{\sqrt{V}}, \, n=0,1,2 \qquad \text{.....................} \qquad (21)$$

$$\Rightarrow \lambda = n\pi\frac{\sqrt{V}}{d} \qquad \text{...............} \qquad \text{..............} \qquad (22)$$

So that we have

$$Ks(Z,t) = AD\,Cos\,n\pi\frac{\sqrt{V}}{d\sqrt{V}}t\;\ell^{\frac{-n^2\pi^2 V}{d^2\phi Kc}Z} \qquad \text{.........................} \qquad (23)$$

$$AD\,Cos\,\frac{n\pi}{d}t\;\ell^{\frac{-n^2\pi^2 V}{d^2\phi Kc}Z} \qquad \text{...............................} \qquad (24)$$

Hence $AD = Kso$

$$Ks = (Z,t) = Kso\, \ell\, \frac{-n^2\pi^2 V}{d^2\phi Kc} Z\ Cos\frac{n\pi}{d}t$$

.... (25)

3. Results and discussion

Results from theoretical values with experimental values on deposition of nitrogen at various formations are presented in tables and figures bellow:

Table 1
Comparison of theoretical and experimental values of deposition of nitrogen at various depths.

Depth	Theoretical values	Experimental values
3	1.17E-03	1.21E-03
6	2.35E-03	2.44E-03
9	3.52E-03	3.34E-03
12	4.70E-03	4.56E-03
15	5.88E-03	5.84E-03
18	7.10E-03	7.44E-03
21	8.23E-03	8.19E-03
24	9.41E-03	9.22E-03
27	1.10E-02	1.14E-02
30	1.20E-02	1.18E-02

Table 2
Comparison of theoretical and experimental values of deposition of nitrogen at various time.

Time per Day	Theoretical values	Experimental values
10	1.17E-03	1.21E-03
20	2.35E-03	2.44E-03
30	3.52E-03	3.34E-03
40	4.70E-03	4.56E-03
50	5.88E-03	5.84E-03
60	7.10E-03	7.44E-03
70	8.23E-03	8.19E-03
80	9.41E-03	9.22E-03
90	1.10E-02	1.14E-02
100	1.20E-02	1.18E-02

Table 3
Comparison of theoretical and experimental values of deposition of nitrogen at various depths.

Depth	Theoretical values	Experimental values
3	1.22E-03	1.28E-03
6	2.42E-03	2.48E-03
9	3.64E-03	3.55E-03
12	4.85E-03	4.77E-03
15	6.07E-03	6.17E-03
18	7.28E-03	7.44E-03
21	8.50E-03	8.44E-03
24	9.71E-03	9.66E-03
27	1.10E-02	1.17E-02
30	1.20E-02	1.25E-02

Table 4
 Comparison of theoretical and experimental values of deposition of nitrogen at various times.

Time per Day	Theoretical values	Experimental values
10	1.22E-03	1.28E-03
20	2.42E-03	2.48E-03
30	3.64E-03	3.55E-03
40	4.85E-03	4.77E-03
50	6.07E-03	6.17E-03
60	7.28E-03	7.44E-03
70	8.50E-03	8.44E-03
80	9.71E-03	9.66E-03
90	1.10E-02	1.17E-02
100	1.20E-02	1.25E-02

Table 5
Comparison of theoretical and experimental values of deposition of nitrogen at various depths.

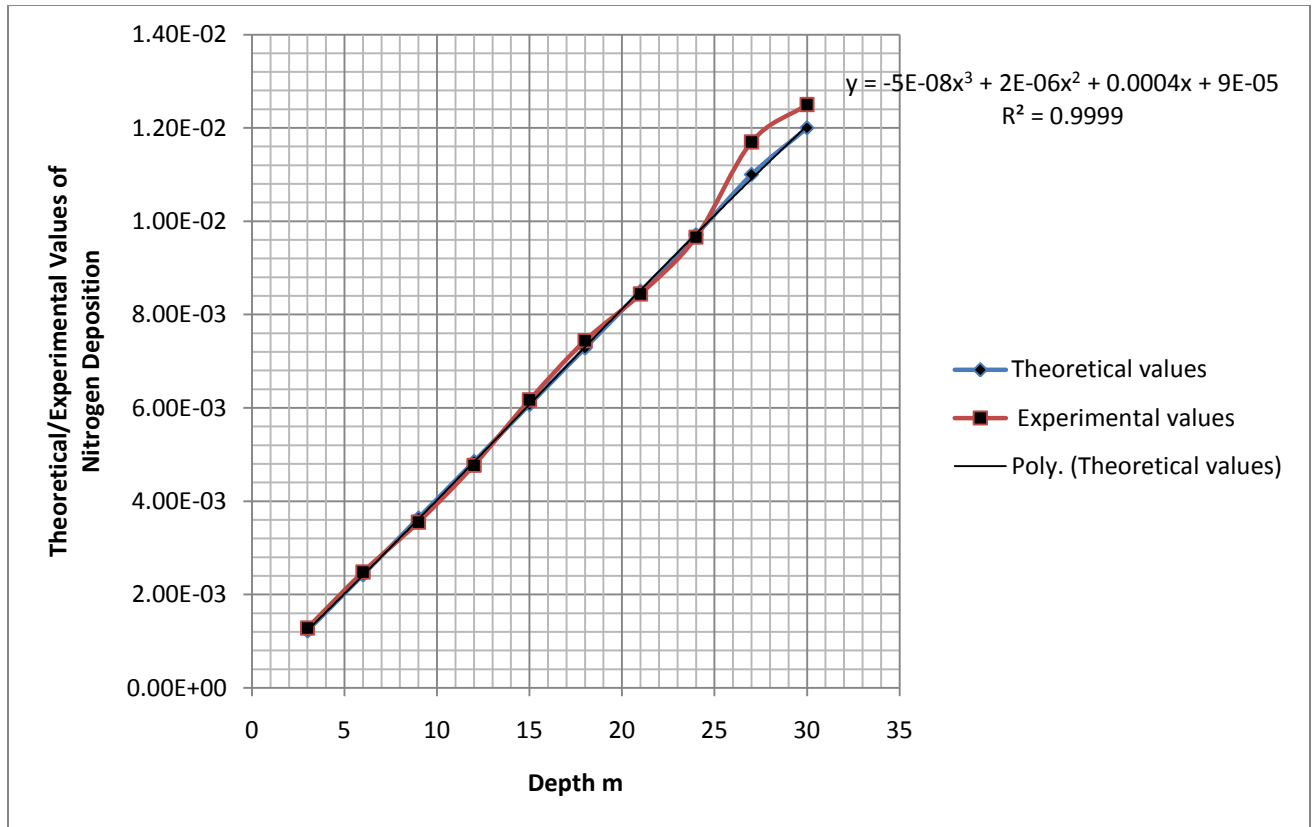| Depth	Theoretical values	Experimental values
3	0.012	0.015
6	0.023	0.026
9	0.035	0.039
12	0.047	0.051
15	0.058	0.061
18	0.071	0.075
21	0.082	0.089
24	0.094	0.099
27	0.11	0.12
30	0.12	0.14

Table 6
Comparison of theoretical and experimental values of deposition of nitrogen at various depths.

Time per Day	Theoretical values	Experimental values
10	0.012	0.015
20	0.023	0.026
30	0.035	0.039
40	0.047	0.051
50	0.058	0.061
60	0.071	0.075
70	0.082	0.089
80	0.094	0.099
90	0.11	0.12
100	0.12	0.14
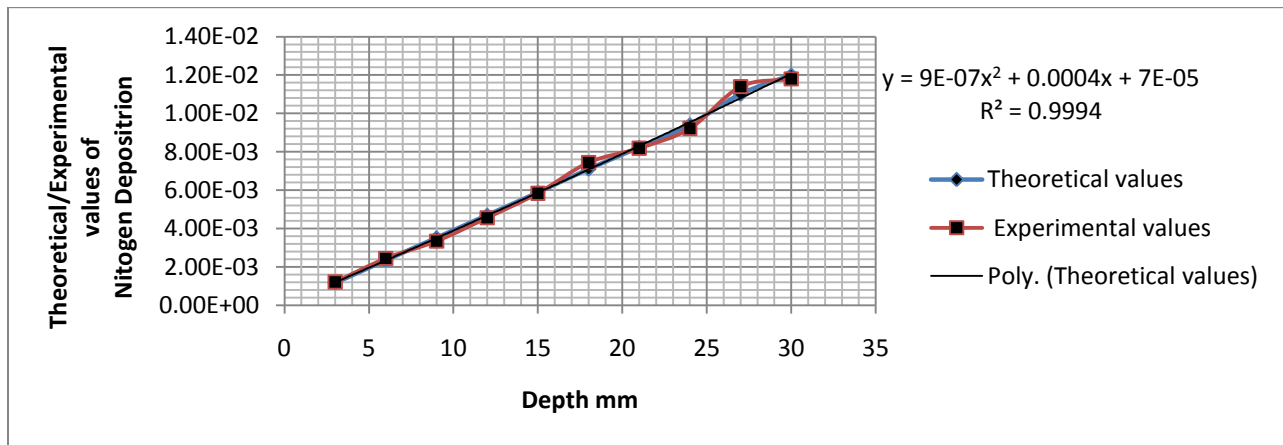
Fig. 1. Comparison of theoretical and experimental values of deposition of nitrogen at various depths.
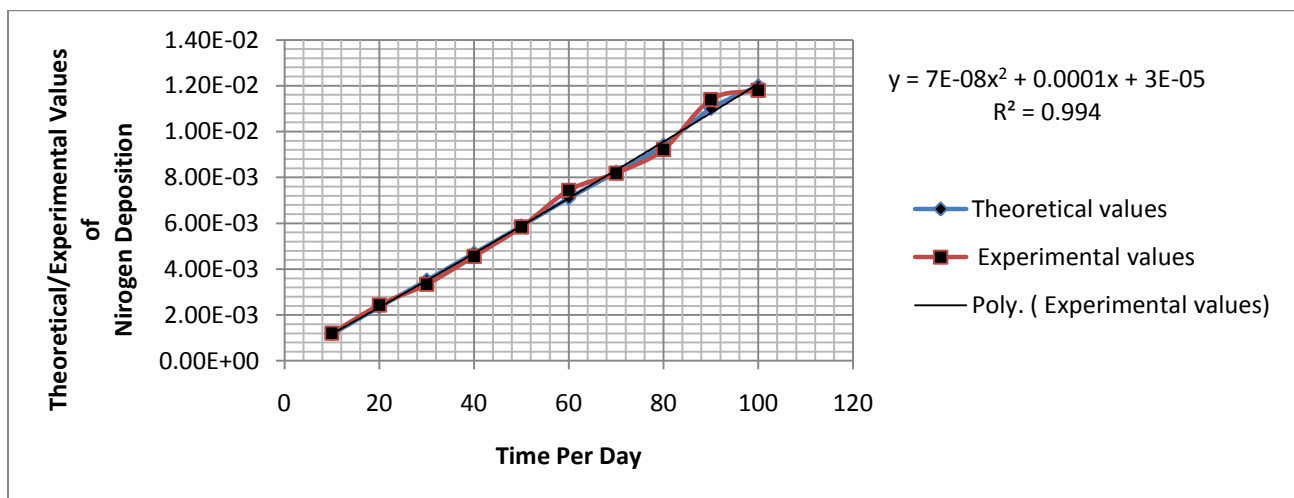
Fig. 2. Comparison of theoretical and experimental values of deposition of nitrogen at various time.

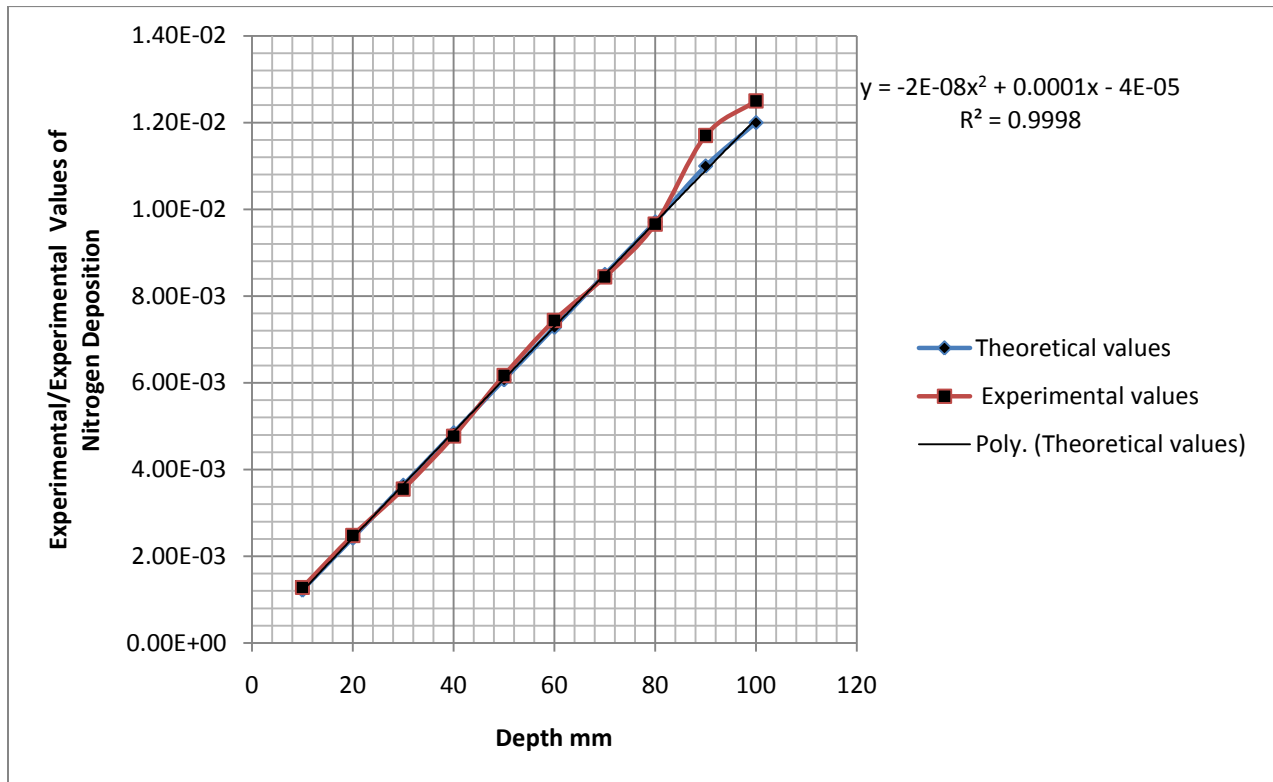**Fig. 3.** Comparison of theoretical and experimental values of deposition of nitrogen at various depths.

Fig. 4. Comparison of theoretical and experimental values of deposition of nitrogen at various depths.
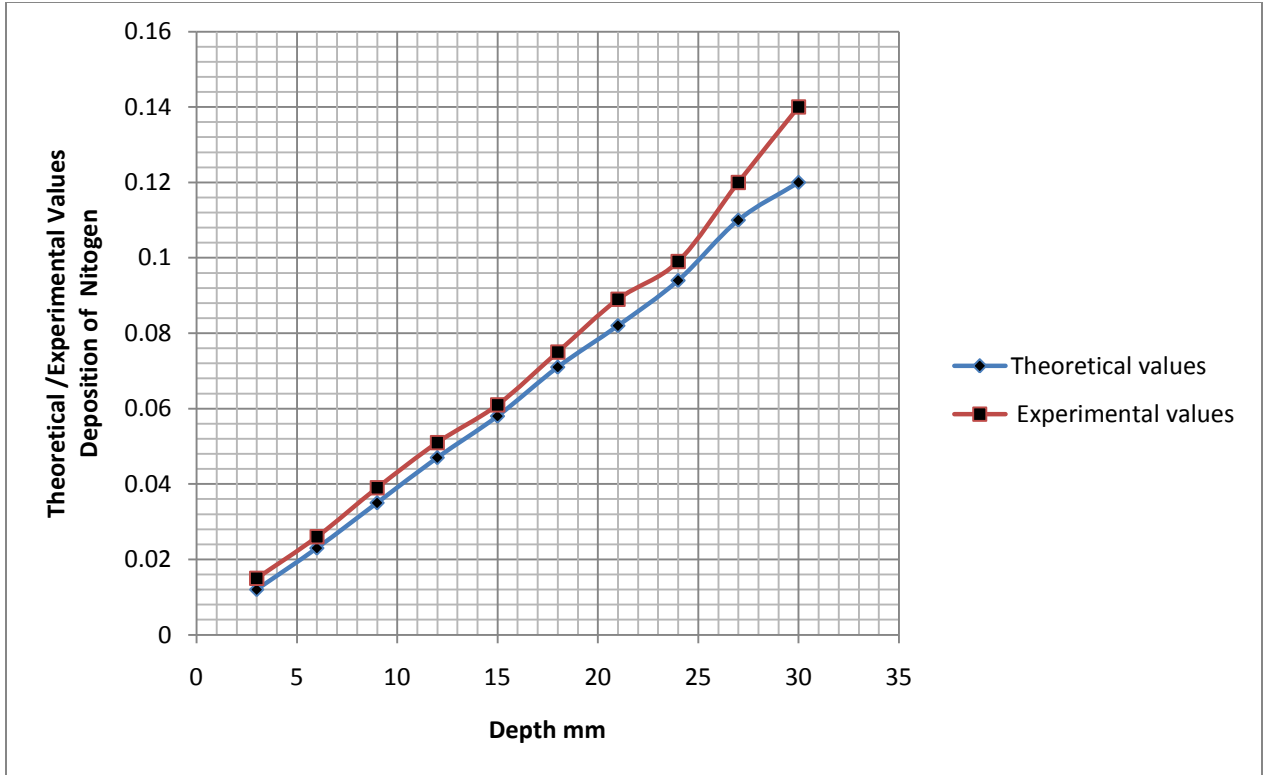
Fig. 5. Comparison of theoretical and experimental values of deposition of nitrogen at various depths.
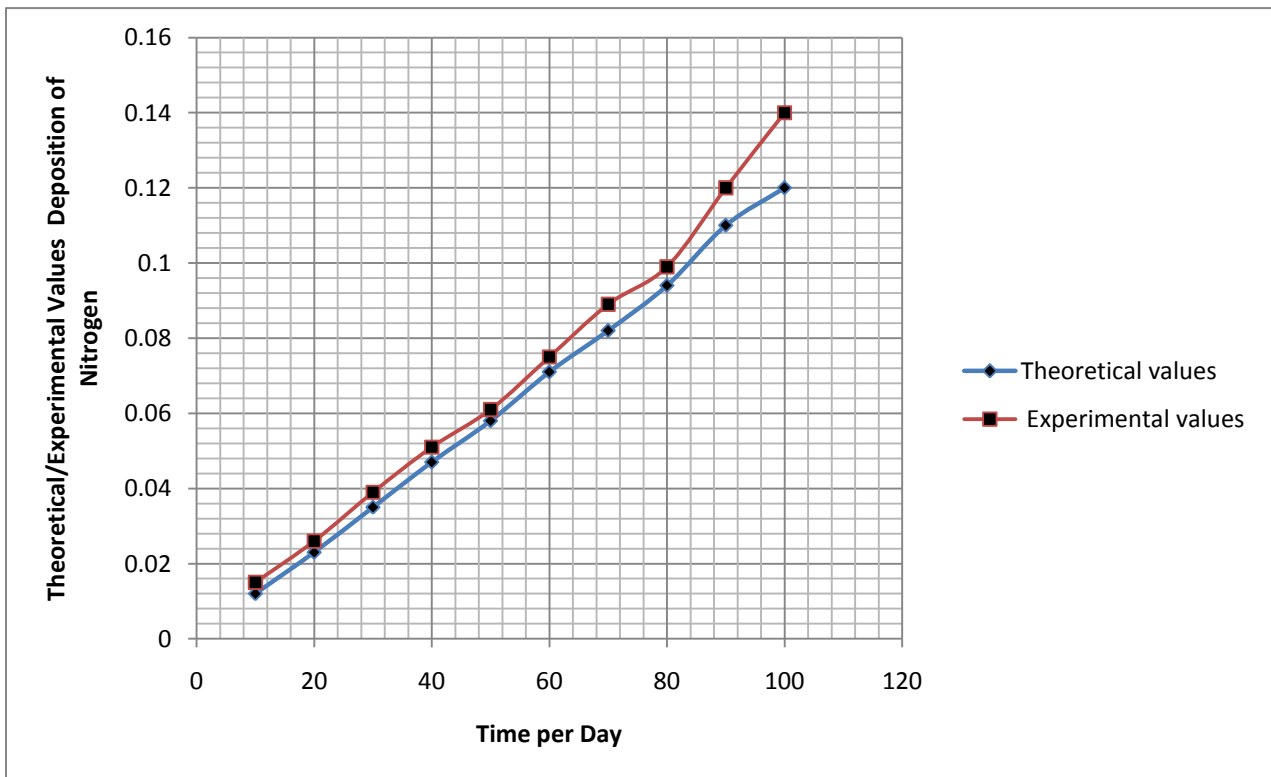

Fig. 1. Comparison of theoretical and experimental values of deposition of nitrogen at various time.

Figure one to five one shows that the theoretical values of the microelements where found to increase from three meters to thirty metres where the optimum values where recorded at the period within ten to hundred days, this condition implies that the microelement developed high concentration from organic soil to fine sand formation in the study area, similar condition where expressed in the experimental values, this condition can be attributed to the geologic history of the study area, meanwhile the formation is in coastal area with high degree of porosity, the substrate utilizations where found to take advantage of high degree of porosity on the increase of the concentration of nitrogen in the study location, the exponential phase of the micronutrients implies that the inhibitor where found to be very low and if microbes where found to deposit in those formation, they would have deposit high concentration in those formation, because it known to be substrate for the microbes to increases in microbial population, high rate of porosity in the formation from the study played a major role on the migration of the nitrogen to ground water aquifers. The study from every point of indication has shows that the inhibitors where found to be insignificant to the deposition of the microelements' in the study location as presented all the figures, which were found to be in exponential phase in the study area, the coastal environment where also found to have contributed to the rate of nitrogen deposition, the developed model developed a best fit with the experimental values, this condition implies that the model can applied to monitor the growth rate of nitrogen deposition in coastal area of port Harcourt.

4. Conclusion

Modeling and simulation to predict the deposition of nitrogen influenced by porosity and inhibition coefficient in coastal area of Port Harcourt has been evaluated, the mathematical model where developed to monitor the rate of nitrogen depositions from organic soil to fine sand formation in the study area. Previous studies where not able to model the behaviour of the microelement under the influence of plug flow application, but the developed equation where able to generate a model that can monitor the migration of nitrogen from organic to fine sand formation. The theoretical and experimental values express an exponential phase of the micronutrient in all the figures presented, at this point it also implies that the concentration of the microelement at the aquiferious zone may definitely developed water pollution in the study area. The condition are expresses from the figures presented, it developed high concentration at the aquiferious zone from 0.014 to 0.14 mg/ that will compared to world health organisation standard if the quality of water in those will be good for consumption..

Reference

Angulo-Jaramillo, R., Moreno, F., Clothier, B.E., Thony, J.L., Vachaud, G., Fernandez-Boy, E., Cayuela, J.A., 1997. Seasonal variation of hydraulic properties of soils measured using a tension disc infiltrometer. Soil Science Society of America Journal 61, 27-32.

Bodner, G., Loiskandl, W., Buchan, G., Kaul, H.P., 2008. Natural and management-induced dynamics of hydraulic conductivity along a cover-cropped field slope. Geoderma 146, 317-325.

Chan, K.Y., Heenan, D.P., Ashley, R., 1994. Seasonal changes in surface aggregate stability under different tillage and crops. Soil and Tillage Research 28, 301-314.

Kodešová, R., Kodeš, V., Žigová, A., Šimunek, J., 2006. Impact of plant roots and soil organisms on soil micro morphology and hydraulic properties. Biologia 61, S339–S343.

Kodešová, R., Kocárek, M., Kodeš, V., Šimunek, J., Kozák, J., 2008. Impact of soil icromorphological features on water flow and herbicide transport in soils. Vadose Zone Journal 7, 798–809.

Kodešová, R., Vignozzi, N., Rohošková, M., Hájková, T., Kocárek, M., Pagliai, M., Kozák, J., Šimunek, J., 2009a. Impact of varying soil structure on transport processes in different diagnostic horizons of three soil types, Journal of Contaminant Hydrology 104, 107-125.

Kodešová, R., Rohošková, M., Žigová, A., 2009b. Comparison of aggregate stability within six soil profiles under conventional tillage using various laboratory tests. Biologia 64, 550-554.

Messing, I., Jarvis, N.J., 1993. Temporal variation in the hydraulic conductivity of a tiled clay soil as measured by tension infiltrometer. Journal of Soil Science 44, 11-24.

Murphy, B.W., Koen, T.B., Jones, B.A., Huxedurp, L.M., 1993. Temporal variation of hydraulic properties for some soils with fragile structure. Australian Journal of Soil Research 31, 179-197.

Petersen, C.T., Hansen, S., Jensen, H.E., 1997. Tillage-induced horizontal periodicity of preferential flow in the root zone. Soil Science Society of America Journal 61, 586-594.

Somaratne, N.M., Smettem, K.R.J., 1993. Effect of cultivation and raindrop impact on the surface hydraulic properties of an alfisol under wheat. Soil and Tillage Research 26, 115-125

Strudley, W.M., Green, T.R., Ascough, I.I.J.C., 2008. Tillage effects on soil hydraulic properties in space and time: State of the science. Soil and Tillage Research 99, 4-48.

Suwardji, P., Eberbach, P.L., 1998. Seasonal changes of physical properties of an Oxic Paleustalf Red Kandosol) after 16 years of direct drilling or conventional cultivation. Soil and Tillage Research 49, 65-77.

Yang, X.M., Wander, M.M., 1998. temporal changes in dry aggregate size and stability. Soil and Tillage Research 49, 173-183.